2019-01-0380

Effects of Perforation Shapes on Water Transport in PEMFC Gas Diffusion Layers

Jiapei Yang[1], Kai H. Luo[2], Xiao Ma[1], Yanfei Li[1] and Shijin Shuai[1]

[1]Tsinghua University, Beijing 100084, China

[2]University College London, Torrington Place, London WC1E 7JE, UK

Abstract

Water management, particularly in the gas diffusion layers (GDL), plays an important role in the performance and reliability of the proton exchange membrane fuel cells (PEMFCs). In this study, a two-phase multiple-relaxation-time (MRT) lattice Boltzmann method (LBM) is employed to simulate water transport in a reconstructed GDL and the effect of perforation shapes is investigated. The revised pseudopotential multiphase model is adopted to realize high-density ratio, good thermodynamic consistency, adjustable surface tension and high contact angle. The transport characteristics are analyzed in both vertical and horizontal transport directions. The LBM simulation provides detailed results in mesoscale and indicates that the surface tension dominates the process of water transport in the perforated GDL, which exhibits unexpectedly similarities in the vertical and horizontal transport. Besides, it is found that the cone-like perforations perform better than cylinder-like perforations as little water clusters together in the bottom of the perforation. Finally, the optimized perforation with defined parameters is derived and discussed, providing guidelines for improving the GDL performance in engineering applications.

Introduction

Over the years, the concern is ever-increasing on air pollution and energy crisis, due to the rapid growth of population and industrialization worldwide [1, 2]. The improvement of conventional engines [3] and the development of new power sources [4] are two typical ways to deal with the energy security and air pollution. The proton exchange membrane fuel cells (PEMFCs) have attracted much attention for their high-efficiency and zero emission. However, water flooding is a critical problem that may restrict the performance, durability and compactness of PEMFCs [4]. Among the components of fuel cell stack, the gas diffusion layer (GDL) plays an important role in guiding air and hydrogen to the catalyst layer for electrochemical reactions. As the product of the electrochemical reaction, liquid water should be removed from GDL properly in time to avoid water blocking in GDL pore, especially in high-current-density conditions. Therefore, proper design of the microstructure for GDL is necessary to enhance the liquid water transport capacity.

Extensive words have been conducted to avoid the occurrence of water flooding in GDL. A laser perforation in GDL was first experimentally examined by Gerteisen et al. [5] in a small testing fuel cell, which had a cylinder shape with diameter 80 μm. The results showed that a better dynamic and comprehensive performance of water removing could be achieved with the perforated GDL. After that, Gerteisen et al. [6] transferred to research on an industrial relevant fuel cell stack to characterize the influences of perforated GDL on flooding phenomena. The experimental results revealed that the water transport capacity in GDL as well as the performance and stability were improved in terms of medium and high current density conditions.

Thus, many experimental measurement techniques in working PEMFC have been developed to observe the water formation and transport in perforated GDL. An optical visualization experiment was conducted by Okuhata et al. [7] and it was found that the liquid water could be effectively reduced and discharged from GDL if the hydrophobic coating on the surface of perforations was not damaged. Similarly, Nishida et al. [8] adopted a cross-sectional visualization technique to investigate the performance enhancement of perforated GDL with hydrophobic channel. They concluded that this combinational structure could promote the through-plane water-removing ability. Except for optical visualization, radiography experiments allowed higher spatial resolution to obtain more information about the internal phenomenon in GDL. The water distribution in perforated GDL with a diameter of about 210 μm was visualized by synchrotron X-ray radiography in the study of Markotter et al. [9]. Their results indicated that the water gathered near the hole while the perforations might change the water distribution. The influences of laser perforation on the water management were also investigated using synchrotron radiography by Alink et al. [10] It was found that GDL would be seriously flooded in high humidification conditions due to the hydrophilic regions of the perforations. Haußmann et al. [11] derived an optimized value for the perforation diameter to avoid flooding effect on the adjacent to the perforation by synchrotron radiography and tomography.

In addition to experimental methods, there are few ways to simulate the process. One of the options simulation way is level-set method. Wang et al. [12] applied level-set method to investigate the water transport characteristics through the perforated GDL. They reported that the optimal diameter of cylinder perforation was 100 μm, which could effectively enhance the water discharge. Another available method is lattice Boltzmann method (LBM). Fang et al. [13] numerically investigated the function relation between the effective transport properties and perforation radius using LBM and also proved that the perforation with larger diameter than the pore size of GDL played a vital role in water transport in perforated GDL.

In consideration of the high costs of experiments and small spatial scale of GDL, the LBM has considerable advantages in contrast to experiments and other conventional simulation methods. The LBM is a powerful technique that can achieve simulation of the pore-scale two-phase flow with complex boundary conditions, in which parallel computing can be easily adopted to offer distinctive computational efficiency [14].

Till now, perforation is limited to cylinder probably due to the manufacture difficulty. However, the liquid water possibly possesses its own unique characteristics if the interface of perforation is tilted for the slant normal direction of interface and un-uniform porosity distribution, which has many potential benefits on water drainage. Therefore, it is necessary to extend the cylinder perforations to cone and other profiled perforations in order to examine their performances on water removing without considering the manufacture difficulties temporarily. This work aims to investigate the effect of perforation shape of GDL on water transport characteristic and water distribution through LBM method and provide guidelines to optimize GDL in engineering operations.

Lattice Boltzmann Method

3D MRT pseudopotential Lattice Boltzmann method

In this work, a D3Q19 LB model with multiple relaxation time (MRT) collision operator is used to simulate the liquid water transport with the complex porous structure GDL. The evolution equation of the distribution function can be written as [15, 16]:

$$f_\alpha(x+e_\alpha\delta_t,t+\delta_t)-f_\alpha(x,t) = -\overline{\Lambda}_{\alpha\beta}(f_\beta-f_\beta^{eq})\big|_{(x,t)}+\delta_t(S_\alpha-0.5\overline{\Lambda}_{\alpha\beta}S_\beta)\big|_{(x,t)} \quad (1)$$

where f_α is the density distribution function, f_α^{eq} is the equilibrium distribution function, x is the position, t is the time, δ_t is the time step, e_α denotes the discrete velocity, $\overline{\Lambda}_{\alpha\beta}=M^{-1}\Lambda M$ is the collision matrix, and Λ represents a diagonal relaxation time matrix :

$$\Lambda = diag(1.0,1.25,1.0,1.0,1.3,1.0,1.3,1.0,1.3,1.25, 1.0,1.25,1.0,1.25,1.25,1.25,1.3,1.3,1.3) \quad (2)$$

In the pseudopotential model, the fluid-fluid interaction force can be expressed as [17, 18]:

$$F_{\sigma,int}(x)=-\psi_\sigma(x)\sum_{\bar{\sigma}}G_{\sigma\bar{\sigma}}\sum_{\alpha=0}^{N-1}w(|e_\alpha|^2)\psi_{\bar{\sigma}}(x+e_\alpha)e_\alpha\delta_t \quad (3)$$

where Ψ is the pseudopotential function coupled with equation of state (EOS) to achieve high density ratio [19] :

$$\psi=\sqrt{\frac{2(P_{EOS}-\rho c_s^2)}{Gc_s^2}} \quad (4)$$

A piecewise linear EOS is adopted in the present paper and the density ratio is 100. In order to achieve a good thermodynamics consistency, Zhang et al. [20] extends an improved forcing scheme developed by Li et al. [21] to D3Q19 lattice, by modifying the second forcing term:

$$\overline{S}_1=\overline{S}_1'+\frac{114\varepsilon F^2}{\psi^2(1/s_1-0.5)} \quad (5)$$

According to Ammar et al. [22], the surface tension can be decoupled from pseudopotential model parameters by adding an extra source term in evolution equation (1).

The fluid-solid interaction force determining the contact angle is vital to porous media due to the immense solid surface area. A modified pseudopotential-based interaction force proposed by Li et al. [23] is adopted in this work to own more accurate contact angle:

$$F_{ads}(x)=-G_w\psi(x)\sum_{\alpha=0}^{N-1}w(|e_\alpha|^2)s(x+e_\alpha)e_\alpha \quad (6)$$

In addition to fluid-fluid interaction force and interaction fluid-solid force, the body force can be introduced through:

$$F_b=-\rho g \quad (7)$$

Computational Domain and Boundary conditions

A 80 × 80 × 80 domain is adopted and each space step represents 3 μm. The reconstruction of GDL is based on the model developed by Schladitz et al. [24]. This model is proposed for the morphological structure of fibrous porous media, and it has been widely adopted to reconstruct GDL by researchers in recent years [25]. GDL consists of straight cylinders (fibers) and binder. In this model, the fibers are randomly placed in the x-y plane through Poisson line process while fibers' anisotropy in height direction is controlled by anisotropy parameter. After the fiber generation, the space near fiber surface is randomly filled with binder. The generation of fibers and binder continues until the porosity reaches the set value. The three-dimension porous media is shown in Figure 1. The diameter of fibers is equal to 8 μm and the porosity is defined as 0.9.

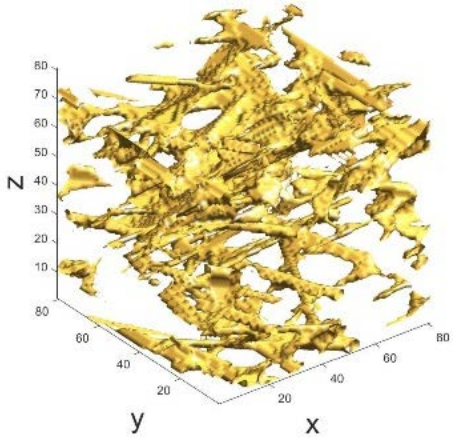

Figure 1. Sketch of the non-perforated GDL.

The schematic and surface equations of test perforations are presented in Figure 2. The cylinder perforation with the diameters of 60 μm (cylinder-like A) is taken as baseline according to previous literature [13]. Following that, a trapezoid cylinder perforation (cylinder-like B) with three-stage cross section is designed to realize tilted interface of perforation with simple processing technology. Obviously, the cone perforation and circular truncated cone perforation (cone-like A and B) are the special cases of trapezoid cylinder perforation by setting the sections of trapezoid cylinder to be infinity. To obtain the detailed effects of tilted interface of perforation on water distribution, this paper also extents the

generation line of cone from straight to parabolic and anti-parabolic (cone-like C and D). Meanwhile, two representations of defect in cylinder perforation of GDL are shown in cylinder-like C and D. For better comparison these various shapes of perforations are classified into cone-like perforations and cylinder-like perforations with four similar perforations shapes for each type based on the principle of same volume. These designs are perforated in the center of GDL while their axle lines are parallel to the z-axis.

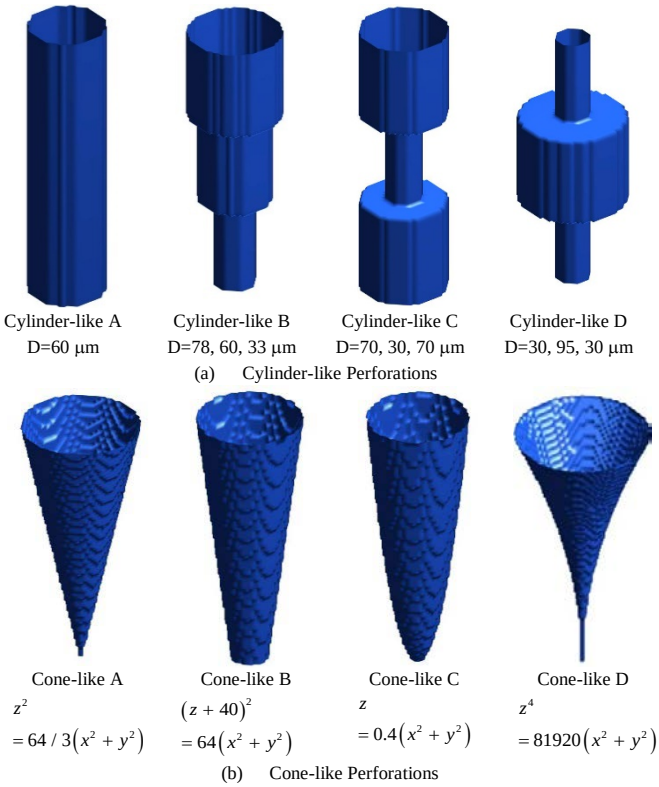

Figure 2. Schematics and surface equations of (a) cylinder-like perforations and (b) cone-like perforations.

In order to simplify the droplet motions in porous with pressure gradient, the body force is applied with the periodic boundary conditions in six directions. The transport characteristics are decomposed into two directions including vertical and horizontal, which are examined to distinguish the water transport capability of GDL with different perforation shapes. In the vertical transport, the body force g is set to be 1e-5 lattice unit (lu) along the z-axis while 108 droplets with diameters of 30 μm are placed randomly in GDL in the initial flooding condition. Except for the body force g along the x-axis, the simulation setups of horizontal transport are the same as the vertical transport.

Validation

To validate the two-phase model used for the present simulation, the surface tension of a droplet is compared with the theoretical one calculated using Young-Laplace law. Figure 3 shows that the simulation results are well consistent with theoretical result no matter what surface tension adjustment factor κ is. The contact angle between static droplet and wall can be changed with contact angel factor Gw. The corresponding relations between contact angle and contact angel factor Gw are indicated in Figure 4. In previous literature it has been indicated that the proper hydrophobic GDL owns better performances on water removing [26]. Hence, the contact angle of in this work is set to 120° for all porous media surfaces to make GDL hydrophobic.

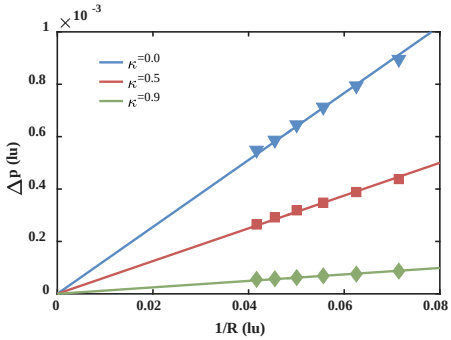

Figure 3. The validation of Young-Laplace law.

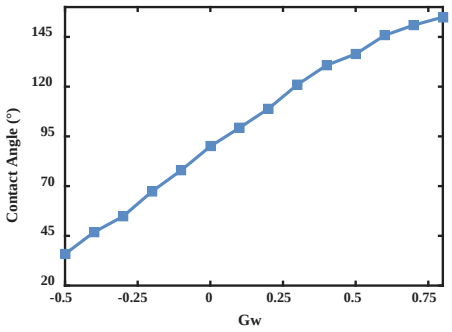

Figure 4. Contact angle of static droplet.

Results

Perforations provide rapid transport for liquid water. Ideally, vast majority of the produced water can be removed through the vertical transport, and the residual water situated inside GDL can be removed by perforation in the horizontal transport [27]. These perforations with slant normal direction of interface cause uneven porosity distribution in vertical and horizontal directions, and these, in turn, lead to the different vertical and horizontal transport characteristics.

The vertical transport

The purpose of vertical transport of water in GDL is to examine the vertical rapid drainage capability with the droplet randomly placed in perforated GDL. Water saturation in perforation is defined as the ratio of the water volume in perforations to the volume of perforations. The perforation has the smaller flow resistance compared to the gap in GDL, resulting in a better water drainage capability in vertical direction. Therefore, the saturation in perforations can be applied to evaluate the water vertical transport capability.

The water saturations in cone-like perforations and cylinder-like perforations in the condition of vertical transport are shown in Figure 5(a) and (b), respectively. Clearly, water amount in perforations has a significant increase initially, but finally saturates when it reaches the threshold. Although the maximum saturation of two perforations is similar in the steady stage, the speed of maximum amount water entering cone-like perforations demonstrates an increase of 5% than

cylinder-like perforations on average. As shown in Figure 6, the lu time of saturation to reach 0.3 of the cone-like perforations is approximate 37% shorter than that of cylinder-like perforations on the whole.

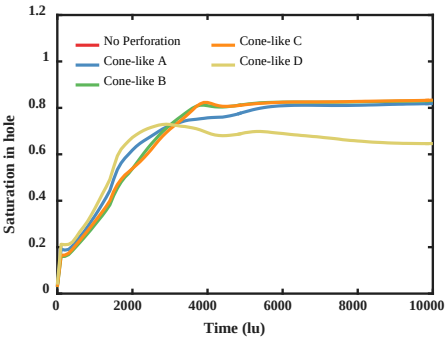

(a) cone-like perforations

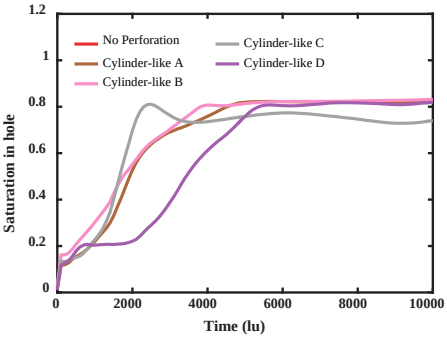

(b) cylinder-like perforations

Figure 5. The relationships between water saturation in perforations and time in the condition of vertical transport.

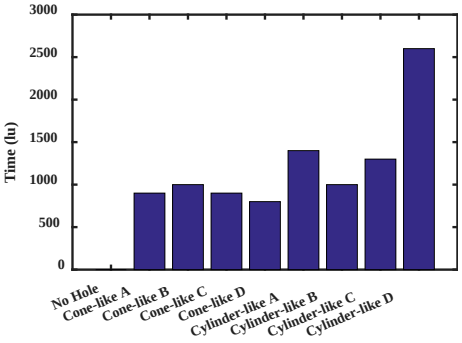

Figure 6. The lu time of saturation to reach 0.3 of different shapes of perforations in the condition of vertical transport.

From Figure 5(a), it can be found that the saturation in cone-like D is much lower than others. This phenomenon can be explained from the results in Figure 7, which presents the evolution of water distribution in the cone-like D case. Herein, the droplet is found to be broken off between the top and bottom of perforation at 4000 lu time, marked by the dark circles. The detailed analysis will be provided in the following section.

The horizontal transport

The Figure 8(a) and (b) illustrate the water saturation in cone-like perforations and cylinder-like perforations in horizontal pressure gradient, respectively. The saturations in two types of perforations increase with the time elapsed, and then become steady after approximate 4000 lu time. However, the maximum saturation in cone-like D is 12% lower than others, similar with the results reported in the previous section. Meanwhile, the saturation for cylinder-like D presents a three-step change before steady state, possibly owing to the three different sections of shape. Figure 9 shows the lu time of saturation to reach 0.3 with different shapes of perforation in horizontal transport. By comparing the lu time of saturation reaching 0.3, the average speed of water coming into the

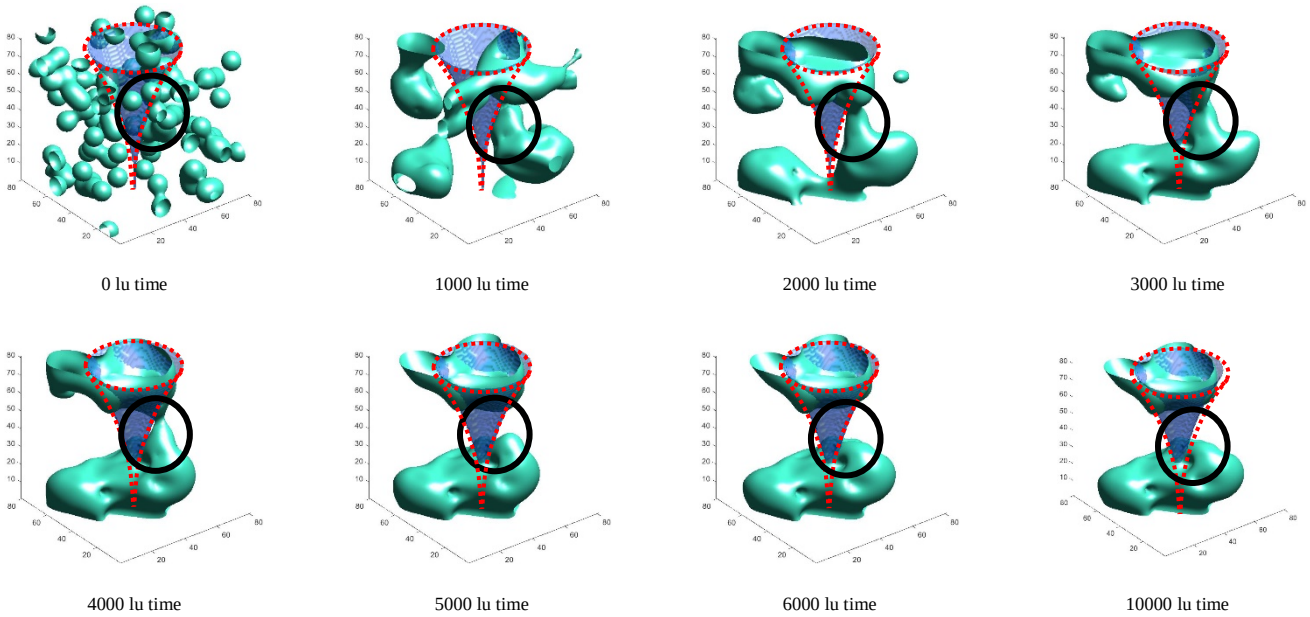

Figure 7. The evolution of water distribution in cone with anti-parabolic generation line (cone-like D). The red dotted line refers to the region of perforation while the green represents droplet.

four cone-like perforations is about 30% higher than the four cylinder-like perforations.

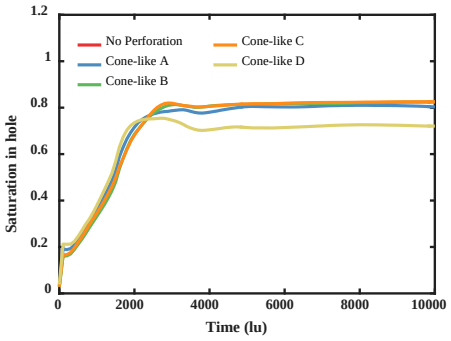

(a) cone-like perforations

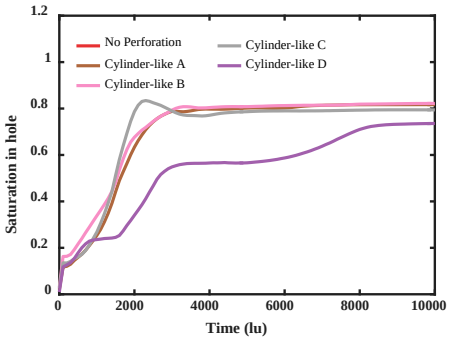

(b) cylinder-like perforations

Figure 8. The relationships between water saturation in perforations and time in the condition of horizontal transport.

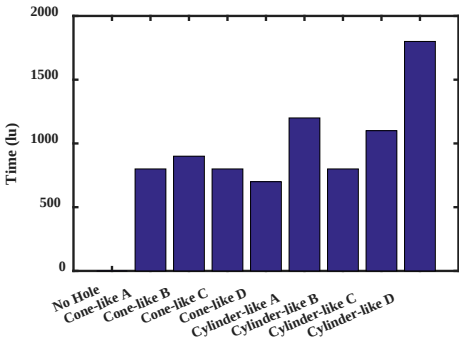

Figure 9. The lu time of saturation to reach 0.3 of different shapes of perforation in the condition of horizontal transport.

The saturations in perforations along with the height at 10000 lu time are presented in Figure 10. It can be clearly seen from Figure 10 that there is a positive correlation between the saturations and the widths of perforations along height direction. Cone-like perforations own small saturation at the bottom of GDL while big saturation at the top of GDL. The saturations in cylinder-like perforation basically stay the same level along height.

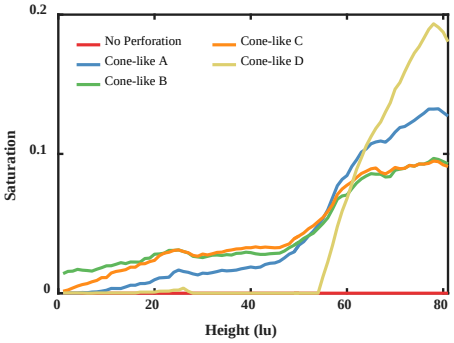

(a) cone-like perforations

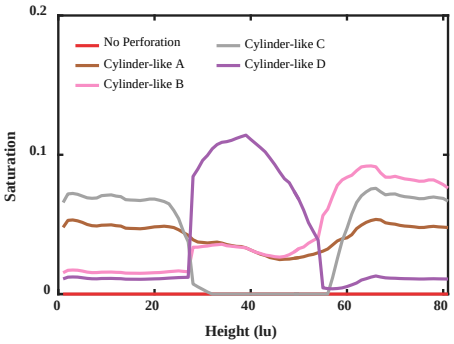

(b) cylinder-like perforations

Figure 10. The saturations in perforations along with the height at 10000 lu time in the condition of horizontal transport.

Discussion

In this present study, water transport was decomposed into vertical and horizontal transport in order to fully understand the transport characteristics of the perforated anisotropic GDL.

From the comparison of the results of vertical and horizontal transport, it is obvious that their transport characteristics are unexpectedly similar with each other. A possible explanation for this might be that the perforation characteristic scale is much larger than the gap among the internal porous media. The randomly distributed small droplets will coalesce to be bigger droplets as a result of the driving force between surface tension and inertia. The droplets will inevitably enter the perforation no matter which direction the pressure gradient point to. After that, the existing water in perforation will continue to grasp the droplets outside of the perforation through surface tension. These effects cause the water gathering mainly around the perforations, which is in agreement with the experimental result of Ref. [9]. Therefore, the vertical and horizontal transport can both lead to water gathering in perforations. Furthermore, the maximum saturation in cone perforation with anti-parabolic generation line (cone-like D) is always lower than other perforations since the dramatic change of cross-sectional area in the axial direction of perforations lead to droplet separation in the middle. In a word, the surface tension dominates the process of water transport in the perforated GDL.

Although the performances of perforation are similar, the results suggest that the cone-like perforations are better than cylinder-like perforations. On one hand, the lateral area of con-like perforations is

larger than that of cylinder-like. The larger the lateral area of perforations, the higher probability for droplets to enter the perforations. This accounts for the faster increasing speed of water saturation in cone-like perforations. On the other hand, the saturation in the bottom of cone-like perforations is much lower than that of cylinder-like perforations. The water clustering together in the bottom of the perforation may block the reactant to reach the catalyst layer, consequently reducing the capability for utilization of catalyst. Based on these two evaluation principles and the faster lu time to reach maximum saturations, the circular truncated cone perforation (cone-like B) should be the best shape of perforation among the shown cases.

Conclusions

In this work, the vertical and horizontal transport characteristics of various perforation shapes in GDL are numerically investigated through 3D MRT LBM, which can realize high density ratio, good thermodynamic consistency, adjustable surface tension and high contact angle. The major results can be summarized as follows:

1. Water can reach perforations through vertical and horizontal transport. It has been identified that the surface tension dominates the process of water transport in perforated GDL, leading to unexpected similar results in the vertical and horizontal transport.
2. Cone-like perforations are superior to cylinder-like perforations due to their larger lateral area and little water clustering at the bottom of the perforation.
3. Overall, the circular truncated cone perforation (cone-like B) is considered as the best shape of perforation among the tested cases.

The greater inertial force effect on water transport in perforations and the optimization of circular truncated cone perforation need further investigation, which are topics of our ongoing works.

References

[1] H. Xu, C. Wang, X. Ma, A.K. Sarangi, A. Weall, J. Krueger-Venus, Fuel injector deposits in direct-injection spark-ignition engines, Progress in Energy and Combustion Science 50 (2015) 63-80.

[2] S. Shuai, X. Ma, Y. Li, Y. Qi, H. Xu, Recent Progress in Automotive Gasoline Direct Injection Engine Technology, Automotive Innovation 1 (2018) 95-113.

[3] X. Ma, F. Zhang, H. Xu, S. Shuai, Throttleless and EGR-controlled stoichiometric combustion in a diesel–gasoline dual-fuel compression ignition engine, Fuel 115 (2014) 765-777.

[4] K. Jiao, X. Li, Water transport in polymer electrolyte membrane fuel cells, Progress in Energy and Combustion Science 37 (2011) 221-291.

[5] D. Gerteisen, T. Heilmann, C. Ziegler, Enhancing liquid water transport by laser perforation of a GDL in a PEM fuel cell, Journal of Power Sources 177 (2008) 348-354.

[6] D. Gerteisen, C. Sadeler, Stability and performance improvement of a polymer electrolyte membrane fuel cell stack by laser perforation of gas diffusion layers, Journal of Power Sources 195 (2010) 5252-5257.

[7] G. Okuhata, T. Tonoike, K. Nishida, S. Tsushima, S. Hirai, Effect of Perforation Structure of Cathode GDL on Liquid Water Removal in PEFC, ECS Transactions 58 (2013) 1047-1057.

[8] K. Nishida, Y. Kono, M. Sato, D. Mizuguchi, Acceleration of Liquid Water Removal from Cathode Electrode of PEFC by Combination of Channel Hydrophilization and Diffusion Medium Perforation, ECS Transactions 75 (2016) 227-236.

[9] H. Markötter, R. Alink, J. Haußmann, K. Dittmann, T. Arlt, F. Wieder, C. Tötzke, M. Klages, C. Reiter, H. Riesemeier, J. Scholta, D. Gerteisen, J. Banhart, I. Manke, Visualization of the water distribution in perforated gas diffusion layers by means of synchrotron X-ray radiography, International Journal of Hydrogen Energy 37 (2012) 7757-7761.

[10] R. Alink, J. Haußmann, H. Markötter, M. Schwager, I. Manke, D. Gerteisen, The influence of porous transport layer modifications on the water management in polymer electrolyte membrane fuel cells, Journal of Power Sources 233 (2013) 358-368.

[11] J. Haußmann, H. Markötter, R. Alink, A. Bauder, K. Dittmann, I. Manke, J. Scholta, Synchrotron radiography and tomography of water transport in perforated gas diffusion media, Journal of Power Sources 239 (2013) 611-622.

[12] X. Wang, S. Chen, Z. Fan, W. Li, S. Wang, X. Li, Y. Zhao, T. Zhu, X. Xie, Laser-perforated gas diffusion layer for promoting liquid water transport in a proton exchange membrane fuel cell, International Journal of Hydrogen Energy 42 (2017) 29995-30003.

[13] W.-Z. Fang, Y.-Q. Tang, L. Chen, Q.-J. Kang, W.-Q. Tao, Influences of the perforation on effective transport properties of gas diffusion layers, International Journal of Heat and Mass Transfer 126 (2018) 243-255.

[14] Q. Li, K.H. Luo, Q.J. Kang, Y.L. He, Q. Chen, Q. Liu, Lattice Boltzmann methods for multiphase flow and phase-change heat transfer, Progress in Energy and Combustion Science 52 (2016) 62-105.

[15] Z. Guo, C. Shu, Lattice Boltzmann method and its applications in engineering, World Scientific2013.

[16] T. Krüger, H. Kusumaatmaja, A. Kuzmin, O. Shardt, G. Silva, E.M. Viggen, The Lattice Boltzmann method : principles and practice, 2017.

[17] X. Shan, H. Chen, Lattice Boltzmann model for simulating flows with multiple phases and components, Physical Review E 47 (1993) 1815-1819.

[18] X. Shan, H. Chen, Simulation of nonideal gases and liquid-gas phase transitions by the lattice Boltzmann equation, Physical Review E 49 (1994) 2941-2948.

[19] P. Yuan, L. Schaefer, Equations of state in a lattice Boltzmann model, Physics of Fluids 18 (2006) 042101.

[20] L. Zhang, Y. Zhu, X. Cheng, Numerical investigation of multi-droplets deposited lines morphology with a multiple-relaxation-time lattice Boltzmann model, Chemical Engineering Science 171 (2017) 534-544.

[21] Q. Li, K.H. Luo, X.J. Li, Lattice Boltzmann modeling of multiphase flows at large density ratio with an improved pseudopotential model, Phys Rev E Stat Nonlin Soft Matter Phys 87 (2013) 053301.

[22] S. Ammar, G. Pernaudat, J.-Y. Trépanier, A multiphase three-dimensional multi-relaxation time (MRT) lattice Boltzmann model with surface tension adjustment, Journal of Computational Physics 343 (2017) 73-91.

[23] Q. Li, K.H. Luo, Q.J. Kang, Q. Chen, Contact angles in the pseudopotential lattice Boltzmann modeling of wetting, Phys Rev E Stat Nonlin Soft Matter Phys 90 (2014) 053301.

[24] K. Schladitz, S. Peters, D. Reinel-Bitzer, A. Wiegmann, J. Ohser, Design of acoustic trim based on geometric modeling and flow simulation for non-woven, Comp Mater Sci 38 (2006) 56-66.

[25] M.H. Shojaeefard, G.R. Molaeimanesh, M. Nazemian, M.R. Moqaddari, A review on microstructure reconstruction of PEM fuel cells porous electrodes for pore scale simulation, International Journal of Hydrogen Energy 41 (2016) 20276-20293.
[26] L. Cindrella, A.M. Kannan, J.F. Lin, K. Saminathan, Y. Ho, C.W. Lin, J. Wertz, Gas diffusion layer for proton exchange membrane fuel cells—A review, Journal of Power Sources 194 (2009) 146-160.
[27] R. Alink, D. Gerteisen, W. Mérida, Investigating the Water Transport in Porous Media for PEMFCs by Liquid Water Visualization in ESEM, Fuel Cells 11 (2011) 481-488.

Contact Information

Corresponding author:

Xiao Ma, Associate Professor

State Key Laboratory of Automotive Safety and Energy

Department of Automotive Engineering

Tsinghua University, Beijing, 100084, China

Tel: +86-13811176872

Email: max@tsinghua.edu.cn

Acknowledgments

This research is supported by the National Key R&D Program of China (No. 2018YFB0105403), Beijing Municipal Science & Technology Commission (No. Z181100004518004) and National Key R&D Program of China“Integration and Control of Fuel Cell Engine for Heavy Duty Truck & Assessment Technologies of Fuel Cell Engine Reliability for Heavy Duty Truck” (面向重型载货车用燃料电池发动机集成与控制 & 重型载货车用燃料电池发动机可靠性测评).

Definitions/Abbreviations

GDL	gas diffusion layers
LBM	lattice Boltzmann method
lu	lattice unit
MRT	multiple relaxation time
PEMFCs	proton exchange membrane fuel cells